Novel High Pressure Phases of β-AlH_3: A Density-Functional Study

P. Vajeeston,* P. Ravindran, and H. Fjellvåg

Center for Materials Science and Nanotechnology, Department of Chemistry, University of Oslo, Box 1033 Blindern N-0315, Oslo, Norway

Received January 29, 2008. Revised Manuscript Received July 21, 2008

Using total energy calculations within the generalized-gradient approximation the high pressure phases, optimized geometry, and electronic structure of AlH_3 are established. Among the 58 structural arrangements considered for the structural optimization calculations, the experimentally known β modification becomes the ground-state structure. Application of pressure makes the sequence of phase transitions from $\beta \rightarrow \alpha' \rightarrow \alpha \rightarrow$ hp1 ($P63/m$) $\rightarrow$ hp2 ($Pm\bar{3}n$) modification and the estimated transition pressures are 2.4, 4.3, 64, and 104 GPa, respectively. The coordination of Al has been changed from six to nine in the newly identified high pressure hp1 and to twelve in hp2 polymorph. The electronic structures reveal that α, α', β, and γ polymorphs are nonmetals with calculated band gap varying between 1.99 and 3.65 eV, whereas the hp1 and hp2 phases possess semiconducting and metallic behavior, respectively.

The current interest in the development of novel metal hydrides stems from their potential use as reversible hydrogen storage devices at low and medium temperatures. Various aluminum based hydrides such as catalyzed sodium Alanate have been recently studied for this purpose. Among them aluminum trihydride (AlH_3) is a very important material because it is one of the byproduct in most of the dehydriding reactions in Al based hydrides. Moreover, it has application as an energetic component in rocket propellants and a reducing agent in alkali batteries and polymerization catalysts. Further, AlH_3 is an unique binary hydride having at least six crystalline phases with different physical properties and at the same time store up to 10.1 wt % of hydrogen.[1] Its gravimetric hydrogen density is two times higher than liquid hydrogen and much higher than that of most of the known metal hydrides. Moreover, elemental Al is a commonly available and recyclable material which could be an acceptable component for the future sustainable society. Thus, it is considered as a possible hydrogen storage material.[2]

The crystal structure of α-AlH_3 has been well studied[3] in the literature, and less attention has been focused on the other polymorphs. Recent theoretical study by Ke et al.[4] found two new phases of AlH_3 which are energetically more favorable than the stable α-modification. Followed by this study Brinks et al.[5,6] and Yartys et al.[7] experimentally solved the structure of α', β, and γ-AlH_3 phases. The structural aspects of irradiated AlH_3 in comparison with the various phases are also investigated in ref 8. Similarly the electronic structure[4,9] and thermodynamic stability[10] of α-AlH_3 are also well studied. The high pressure study by Graetz et al.[11] observed no pressure induced structural transition in AlH_3 up to at least 7 GPa, which is consistent with earlier high pressure studies.[12,13] The pressure dependence on the electronic structure is also discussed in ref 11. During revision of this article, a recent high pressure study by Goncharenko et al. has come to the attention of the authors, in which application of pressure on α-modification transforms it into two different modifications hp1 and cubic hp2 phase at ca. 60 and 100 GPa, respectively (the structure of the hp1 phase has not yet been solved experimentally).[14] As the high pressure diffraction studies are unable to identify the exact positions of hydrogen atoms owing to its very low scattering cross section, theoretical knowledge about its stability at high pressure is very important. The present type of theoretical investigations are highly successful[15,16] to predict a series of pressure-induced structural transitions in MgH_2 and other

* E-mail: ponniahv@kjemi.uio.no. Homepage: http://www.folk.uio.no/ponniahv.

(1) Brower, F. M.; Matzek, N. E.; Reigler, P. F.; Rinn, H. W.; Roberts, C. B.; Schmidt, D. L.; Snover, J. A.; Terada, K. *J. Am. Chem. Soc.* **1976**, *98*, 2450.
(2) Schlapbach, L.; Züttel, A. *Nature* **2001**, *414*, 353–358.
(3) Turley, J. W.; Rinn, H. W. *Inorg. Chem.* **1969**, *8*, 18–22.
(4) Ke, X.; Kuwabara, A.; Tanaka, I. *Phys. Rev. B* **2005**, *71*, 184107–184113.
(5) Brinks, H. W.; Istad-Lem, A.; Hauback, B. C. *J. Phys. Chem. B* **2006**, *110*, 25833–25837.
(6) Brinks, H. W.; Langley, W.; Jensen, C. M.; Graetz, J.; Reilly, J. J.; Hauback, B. C. *J. Alloys Compd.* **2006**, *433*, 180–183.
(7) Yartys, V. A.; Denys, R. V.; Maehlen, J. P.; Frommen, C.; Fichtner, M.; Bulychev, B. M.; Emerich, H. *Inorg. Chem.* **2007**, *46*, 1051–1055.
(8) Zogal, O. J.; Vajda, P.; Beuneu, F.; Pietraszko, A. *Eur. Phys. J. B* **1998**, *2*, 451–456.
(9) Aguayo, A.; Singh, D. J. *Phys. Rev. B* **2004**, *69*, 155103–155107.
(10) Wolverton, C.; Ozolins, V.; Asta, M. *Phys. Rev. B* **2004**, *69*, 144109–144125.
(11) Graetz, J.; Chaudhuri, S.; Lee, Y.; Vogt, T.; Muckerman, J. T.; Reilly, J. *Phys. Rev. B* **2006**, *74*, 214114–214121.
(12) Baranowski, B.; Hochheimer, H. D.; Strossner, K.; Honle, W. *J. Less-Common Met.* **1985**, *113*, 341–347.
(13) Goncharenko, I. N.; Glazkov, V. P.; Irodova, A. V.; Somenkov, V. A. *Physica B* **1991**, *174*, 117–120.
(14) Goncharenko, I.; Eremets, M. I.; Hanfland, M.; Tse, J. S.; Amboage, M.; Yao, Y.; Trojan, I. A. *Phys. Rev. Lett.* **2008**, *100*, 045504−4.
(15) Vajeeston, P.; Ravindran, P.; Fjellvåg, H.; Kjekshus, A. *J. Alloys Compd.* **2003**, *363*, L7–11; *Appl. Phys. Lett.* **2003**, *82*, 2257−2259; *Phys. Rev. Lett.* **2002**, *89*, 175506−175509.
(16) Vajeeston, P.; Ravindran, P.; Hauback, B. C.; Fjellvåg, H.; Furuseth,S.; Hanfland, M.; Kjekshus, A. *Phys. Rev. B* **2006**, *73*, 224102–224109.

10.1021/cm800282b CCC: $40.75
Published on Web 08/30/2008

hydrogen storage materials. Hence, we have studied the structural phase stability of AlH_3 at high pressures in this article.

Total energies have been calculated by the projected-augmented plane-wave (PAW)[17] implementation of the Vienna ab initio simulation package (VASP).[18] All these calculations are made with the generalized gradient approximation of the PBE (PBE-GGA)[19] exchange correlation functional and the projector augmented wave method. It should be noted that both PW91[20] and PBE functionals gave almost same result. The differences in the energetics and structures of using these two functionals were found to be negligible, and the results reported here were computed with the PBE functional. Ground-state geometries were determined by minimizing stresses and Hellman−Feynman forces using the conjugate-gradient algorithm with force convergence less than 10^{-3} eV/Å. Brillouin zone integration was performed with a Gaussian broadening of 0.1 eV during all relaxations. In order to span a wide range of energetically accessible crystal structures, unit-cell volume and shape as well as atomic positions were relaxed simultaneously, in a series of calculations made with progressively increasing precision. A final high accuracy calculation of the total energy was performed after completion of the relaxations with respect to **k**-point convergence and plane-wave cutoff. From various sets of calculations, it was found that 600 **k** points in the whole Brillouin zone for the α-AlH_3 structure with a 500 eV plane-wave cutoff are sufficient to ensure optimum accuracy in the computed results. The **k** points were generated using the Monkhorst−Pack method with a grid size of 10 × 10 × 6 for structural optimization. A similar density of **k** points and energy cutoff were used to estimate total energy as a function of volume for all the structures considered for the present study. Iterative relaxation of atomic positions was stopped when the change in total energy between successive steps was less than 1 meV/cell.

The following 58 potentially applicable structure types have been used as inputs in the structural optimization calculations (alphabetical order with Pearson structure-classification notation in parenthesis): AgN_3 (oI16), AlD_3 (hR8), γ-AlH_3,[7] AlF_3 (hR8), AlF_3-p321(hP12), AlF_3 (tP64), $AlOH_3$ (aP14), β-AlF_3 (oS48), Au_2Br_6 (mP32), AuF_3 (hP24), BF_3 (aP32), BF_3 (mP32), BiF_3 (oP16), BiI_3 (hP8), BrF_3 (oS16), $CfCl_3$ (oS16), $CrBr_3$ (hP24), CrO_3 (oS16), MoO_3 (oS17), FeF_3 (hR8), β-FeF_3 (cF64), GaF_3 (hR8), $GdBr_3$ (mS16), HoD_3 (hP24), IF_3 (oP16), InF_3 (hR8), $IrAs_3$ (cI32), KN_3 (tI16), LaF_3 (hP24), β-LaF_3 (hP24), $MoBr_3$ (oP16), NCl_3 (oP48), NaO_3 (oI8), $NdOH_3$ (hP14), NiF_3 (hR8), PBr_3 (oP16), PH_3O_3 (oP56), PO_3PuF_3 (hP8), RbN_3 (tP4), S_3O_9 (oP48), $Sb_2O_5H_2O$ (cF80), $SbCl_3$ (oP16), SbF_3 (oS16), ScF_3 (hR4), $(SeO_3)_4$ (tP32), ThI_3 (oS64), TiF_3 (hR4), UI_3 (oS16), γ-UO_3 (tI64), α-UO_3 (oS8), UO_3 (oS8), UO_3 (oF128), WO_3 (hP12), ε-WO_3 (mP16), WO_3 (tP16), WO_3 (oP32), YF_3 (cP12), YbH_3 (cF16), and ZrI_3 (hP8).[21] It should be noted that during the structural optimization some of the initial structures are converted into other high symmetry structure types and hence they are not included in the above list. The calculated total energy as a function of volume has been fitted to the so-called universal equation of state (EOS)[22] to calculate the bulk modulus (B_0), its pressure derivative (B_0') and also to generate the pressure−volume curves. The EOS for different phases are also independently verified by fitting the total energy to six other EOSs. The transition pressures are calculated from the pressure vs Gibbs free energy curves. The Gibbs free energy ($G = U + PV - TS$ where $T = 0$; G = total energy + pressure × volume) is calculated in the following way:

The calculated volume verses total energy for two data sets were read in, and for each data set, the total energy and volume have been fitted to the universal EOS function.[22] The pressure is defined as $p = (B_0/B_0')[(v_e/v)^{B_0'} - 1]$, which gives volume ($v$) = $v_e/((1 + (B_0'/B_0p)^{(1/B_0')}$ where v_e, B_0, and B_0' refer to the equilibrium volume, bulk modulus, and derivative of the bulk modulus, respectively. The inverse is then calculated using the bisection method. From the scan over the pressures, the corresponding difference in the enthalpy between the two data sets was calculated.

Among the considered structures, the β-FeF_3-type atomic arrangement is found to have the lowest total energy (referred to hereafter as β-AlH_3). The calculated positional and lattice parameters are found to be in good agreement (see Table 1) with recent experimental findings by Brinks et al.[6] and theoretical work by Ke et al.[4] This phase consists of corner-sharing AlH_6 octahedra. The octahedra are almost regular with Θ_{H-Al-H} = 87.2−92.8° and Al−H distances of 1.724 Å. Few other structural modifications are found to be energetically closer to the β phase, and these are omitted in Figure 2 for the sake of clarity. The next energetically favorable phase is orthorhombic β-AlF_3-type (space group *Cmcm*; α′-AlH_3) atomic arrangement, and the involved energy difference between this phase with β-AlH_3 at the equilibrium volume is only ca. 32.6 meV/fu (see Figure 2). The calculated structural parameters are found to be in good agreement (see Table 1) with the recent experimental finding.[5] The α′-AlH_3 structure consists of AlH_6 octahedra where all hydrogen atoms are shared between two octahedra. This corner-sharing network is more open than that in α-AlH_3, giving rise to hexagonal shaped pores with a diameter of ca. 3.6 Å. As a result, the volume per AlH_3 unit at equilibrium is increased from ca. 33.5 $Å^3$ in α to 39.3 $Å^3$ in α′-AlH_3. The calculated average Al−H distance is 1.72 Å, and the Θ_{H-Al-H} varies from 87.2 to 92.8°.

Yartys et al.[7] solved the structure of γ modification and found that it has an orthorhombic structure with the space group *Pnnm*. But this γ modification is found to be 30 meV/fu higher in energy than α′-AlH_3 at equilibrium volume. This γ phase contains two different types of octahedra sharing their vertices and edges. These octahedra are connected

(17) (a) Blöchl, P. E. *Phys. Rev. B* **1994**, *50*, 17953–17979. (b) Kresse, G.; Joubert, J. *Phys. Rev. B* **1999**, *59*, 1758–1775.
(18) (a) Kresse, G.; Hafner, J. *Phys. Rev. B* **1993**, *47*, R558–561. (b) Kresse, G.; Furthmuller, J. *Comput. Mater. Sci.* **1996**, *6*, 15–50.
(19) Perdew, J. P.; Burke, S.; Ernzerhof, M. *Phys. Rev. Lett.* **1996**, *77*, 3865–3868.
(20) Perdew, J. P.; Chevary, J. A.; Vosko, S. H.; Jackson, K. A.; Pederson, M. R.; Singh, D. J.; Fiolhais, C. *Phys. Rev. B* **1992**, *46*, 6671.
(21) *Inorganic Crystal Structure Database*; Gmelin Institut: Germany, 2006.
(22) Vinet, P.; Rose, J. H.; Ferrante, J.; Smith, J. R. *J. Phys.: Condens. Matter* **1989**, *1*, 1941–1963.

Table 1. Optimized Structural Parameters, Bulk Modulus (B_0), Pressure Derivative of Bulk Modulus (B_0'), and Calculated Energy Band Gap for AlH$_3$ Polymorphs

phase (space group)	cell constants (Å)	sites: positional parameters	B_0 (GPa)	B_0'	E_g (eV)
α-AlH$_3$	a = 4.492 (4.4493)[a]	Al(6*b*): 0, 0, 0	28	5.4	2.34
($R\bar{3}c$)	c = 11.821 (11.8037)[a]	H (18*e*): (0.628),[a] 0, $^1/_4$			
α′-AlH$_3$	a = 6.523 (6.470)[b]	Al1(4*a*): 0, $^1/_2$, 0; Al2(8*d*): $^1/_4$, $^1/_4$, 0	27	4.5	4.1
(β-AlF$_3$-type; *Cmcm*)	b = 11.139 (11.117)[b]	H1(8*f*): 0, 0.2138, 0.4453 (0, 0.197, 0.451)[b]			
	c = 6.604 (6.562)[b]	H2(16*h*): 0.3094, 0.1024, 0.0492 (0.312, 0.100, 0.047)[b]			
		H3(4 *c*): 0, 0.4571, $^1/_4$ (0, 0.465, $^1/_4$)[b]			
		H4(8*g*): 0.2071, 0.2853, $^1/_4$ (0.298, 0.277, $^1/_4$)[b]			
β-AlH$_3$	a = 9.065 (9.0037)[c]	Al(16*d*): $^1/_2$, 0, 0	34	2.5	3.22
($Fd\bar{3}m$)		H(48*f*): 0.4306 (0.4301),[c] $^1/_8$, $^1/_8$			
γ-AlH$_3$	a = 5.4560 (5.3806)[d]	Al1(2*b*): 0, 0, $^1/_2$; Al2(4*g*): 0.789, 0.085, 0 (0.7875, 0.0849, 0)[d]	42	2.1	3.24
(*Pnnm*, 58)	b = 7.4038 (7.3555)[d]	H1(2*d*): 0, $^1/_2$, $^1/_2$			
	c = 5.8005 (5.77511)[d]	H2(4*g*): 0.653, 0.299, 0 (0.626, 0.278, 0)[d]			
		H3(4*g*): 0.0977, 0.1382, 0 (0.094, 0.130, 0)[d]			
		H2(8*h*): 0.7991, 0.0834, 0.2979 (0.762, 0.078, 0.309)[d]			
hp1-AlH$_3$	a = 5.3845 (4.0444)[e]	Al(2*d*): $^2/_3$, $^1/_3$, $^1/_4$	43	8.1	1.99
(NdOH$_3$, *P*63/*m*)	c = 2.4840 (2.5049)[e]	H(6*h*): 0.6554, 0.7373, $^1/_4$ (0.5909, 0.6986, $^1/_4$)[e]			
hp2-AlH$_3$	a = 3.0768[e]	Al(1*a*): 0, 0, 0	39	6.2	
proto type; $Pm\bar{3}n$)		H(3*c*): $^1/_4$, 0, $^1/_2$			

[a] Experimental value from ref 3. [b] Experimental value from ref 5. [c] Experimental value from ref 6. [d] Experimental value from ref 7. [e] At the phase transition point.

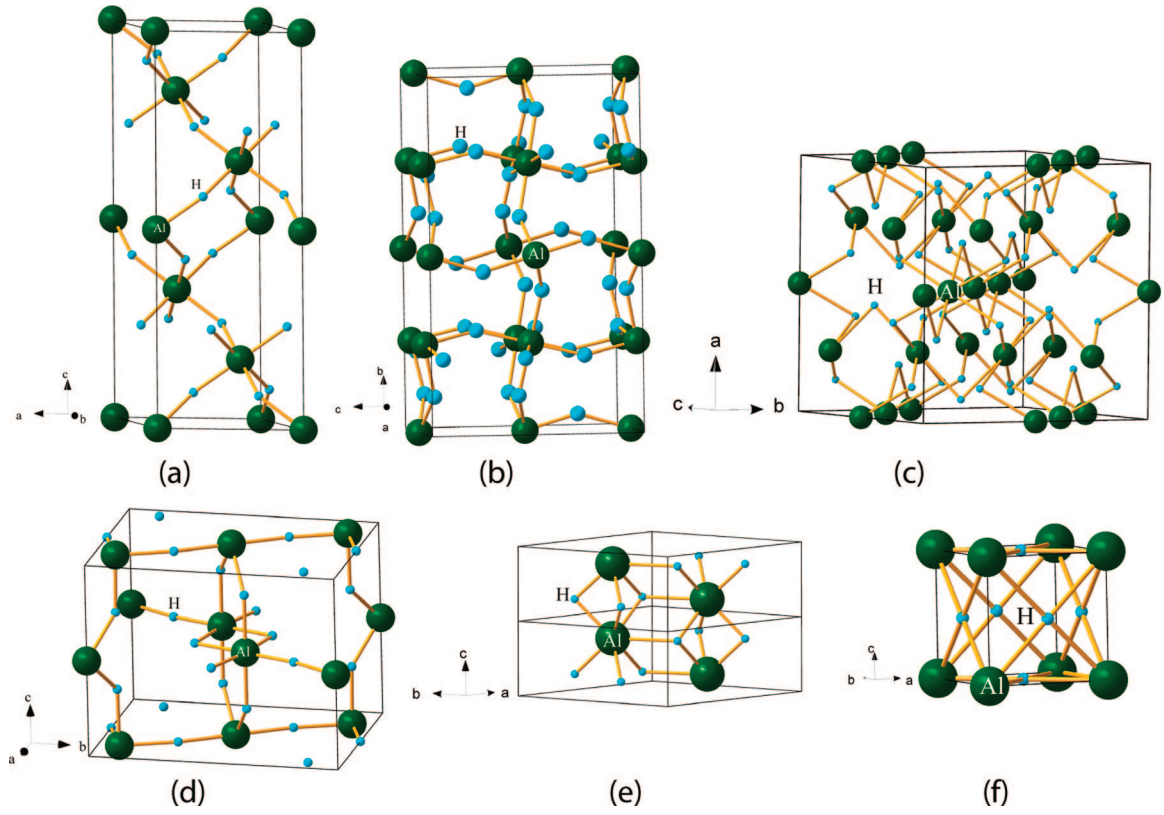

Figure 1. Crystal structures of AlH$_3$ in (a) α-AlH$_3$, (b) α′-AlH$_3$, (c) β-AlH$_3$, (d) γ-AlH$_3$ phases, and the newly identified high pressure modifications such as (e) NdOH$_3$ derived-hp1 (*P*63/*m*) and (f) cubic hp2 ($Pm\bar{3}n$) phases.

in such a way that they have a hydrogen-bridge bond formation which is different than those in other known polymorphs. The calculated Al−H distances within this structure vary between 1.72 and 1.77 Å, and the H−Al−H angle varies from 86 to 94°. As the γ phase is higher in energy than the other polymorphs in the whole volume range, it may be experimentally stabilized by temperature. Similar to the α′ modification, γ modification also has open pores. Hence, both modifications have almost similar equilibrium volumes (Figure 2b). The next energetically favorable structure is α-AlH$_3$ that consisting of corner-shared octahedra and building a distorted primitive Al sublattice. In this phase, the Al−H distance at the equilibrium is 1.72 Å and the H−Al−H angle is almost 90°. The involved energy difference between the α- and β-AlH$_3$ phase is found to be only 32.6 meV/fu. It is interesting to note that the involved energy difference between the α, α′, β, and γ-AlH$_3$ is very small, and hence, one can easily modify one polymorph into another by application of temperature or pressure. One should also remember that the calculated results are valid only for low temperatures. However, the experimental findings

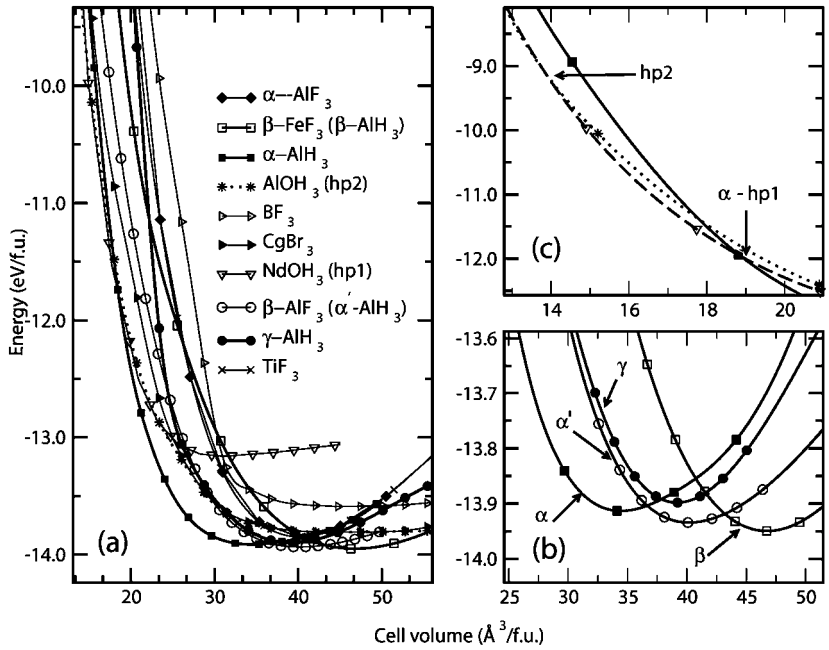

Figure 2. (a) Calculated volume versus total energy curves for AlH_3. Magnified versions of the corresponding transition points are shown in parts b and c.

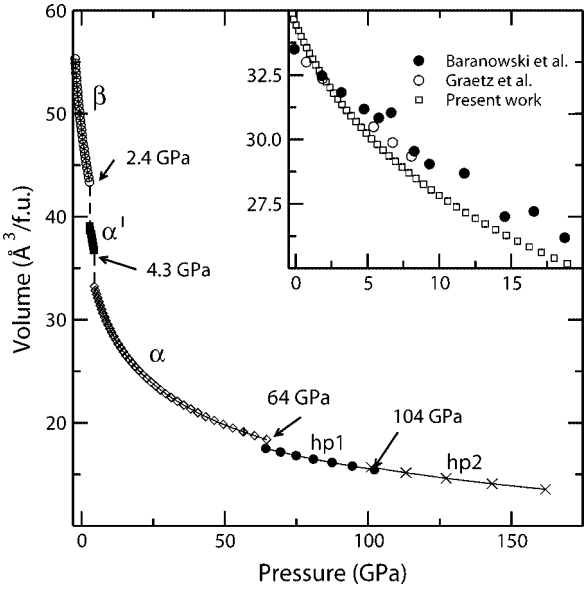

Figure 3. Estimated pressure vs volume curve for AlH_3 and the transition pressures are marked by arrows. The inset figure shows the calculated pressure vs volume curve for the α polymorph with the corresponding experimental observations by Baranowski et al.[12] and Graetz et al.[11]

show that depending upon the synthesis route/conditions one can stabilize different polymorphs of AlH_3.[3,5−7]

Our previous experience on MgH_2 shows that the transition pressures (including structural transition sequence) are not very sensitive to temperature effect and the transition pressures are overall underestimated by ∼2 GPa.[16] As discussed above, β-AlH_3 is the ground-state structure and it transforms into α′ modification at 2.4 GPa (see Figures 2 and 3). Further application of pressure on this α′ modification transforms into α modification at 4.3 GPa. This α modification is experimentally found to be the most stable structure at ambient condition and one can store it for several years without losing H_2.[3] It should be noted that the estimated volume discontinuities at the transition points between the β to α′ to α phases are 7 and 4.3 Å^3/fu, respectively (see Figure 3). This indicates that these structural transitions are originating from the diffusion of atoms. On comparing the equilibrium volumes of the above-mentioned three phases, we found that one can store same quantity of hydrogen with 26% more volume efficiency in the α phase than that in the β phase. Because of the compact atomic arrangement and small pore size, α modification becomes very stable compared to the other modifications.

Further application of pressure shows that the α modification transforms into a $NdOH_3$ derived modification [see Figure 2b; hp1-AlH_3 (*P*63/*m*) modification] around 64 GPa. The estimated volume discontinuity at this transition point is 3.7 Å^3/fu. In this phase, Al coordination is changed from 6 to 9 and the Al−H distance varies within this structure from 1.66 to 1.73 Å (Figure 1e). Recently, ref 14 reported that the hp1 phase can be either monoclinic or trigonal. On the other hand, recent theoretical investigation by Pickard et al.[23] shows that the hp1-phase is orthorhombic (*Pnma*). But, our finding shows that the hp1 phase rather has a hexagonal (*P*63/*m*) structure with the lowest energy among all these phases and the orthorhombic (*Pnma*) structure suggested in ref 23 is energetically closer to the presently predicted *P*63/*m* structure. The increase of pressure above 104 GPa brings up a new cubic polymorph (see Table 1; hp2-AlH_3 modification) which is consistent with recent experimental findings.[14] In this hp2 modification, each Al is surrounded by 12 H atoms, and as a result, it consists of a AlH_{12} cuboctahedral arrangement. This hp2 phase has very short H−H separation ever observed in any metal/nonmetal hydrides, except molecular hydrogen. Usually by the loss of covalency with pressure, one could expect increase in coordination number and also high symmetry structures as

(23) Pickard, C. J.; Needs, R. J. *Phys. Rev. B* **2007**, *76*, 144114–5.

we have found in AlH_3. We have also made lattice dynamical calculations for all the high pressure phases of AlH_3 and found no negative phonon frequencies indicating that all these phases are expected to be thermodynamically stable. So, one can conclude that the presently predicted hp1 (*P*63/*m*) phase should be the intermediate pressure phase, observed experimentally from high pressure measurements.[14]

The calculated bulk modulus (see Table 1) values varies between 28 to 42 GPa for the different polymorphs of AlH_3. Among the identified phases, α-AlH_3 has the smallest B_0 value and the P63/*m* (hp1-AlH_3) modification has the highest value. The equilibrium volumes for these phases are in the range of 31.19−46.81 Å^3/fu (see Table 1). It is worthwhile to note that, for the α phase, the experimentally derived B_0 value varies between 42 and 49 ± 4 GPa.[11,12,14] The theoretical values presented in ref 11 are found to be closer to the experimental values. However, present theoretical study shows that, even though the calculated equilibrium volumes are very close to the experimental and other theoretical values, the calculated B_0 value is almost half. In order to verify the predicted B_0 values for different phases of AlH_3 using universal EOS, we have fitted the total energy vs volume curve to six other EOS and arrived at almost the same B_0 values given in Table 1. However, it can be noted that the simulated pressure−volume curve for the α phase is almost identical to the experimental curves of Baranowski et al.[12] and Graetz et al. (see inset of Figure 3). It may be recalled that from the present type of theoretical calculation one can reliably reproduce the B_0 within 5 GPa accuracy.[16] An independent high pressure measurement for high quality samples at low temperature is recommended to clarify this discrepancy. Further, the interaction between moleculelike AlH_3 structural subunits has van der Waals-like weak secondary bonding which can not be properly described by the present type of calculations and this could also explain the discrepancy.

The total density of states (DOS) at the equilibrium volumes for the α, α′, *β*, and *γ* and DOS at the transition point for hp1 (P63/*m*), and hp2 ($Pm\bar{3}n$) modifications of AlH_3 are displayed in Figure 4. All modifications (except hp2) have finite energy gap (E_g; from 1.99 to 3.65 eV for the α, α′, *β*, and *γ*) between the valence band (VB) and the conduction band (CB), and hence, they are nonmetals. According to textbook chemistry, the insulating behavior can be explained as follows: for each AlH_3, three electrons from Al fill the three originally half-filled H s orbitals resulting in a complete filling of the VB and accordingly leading to insulating behavior. However, it is well-known that standard density functionals, such as the PBE-GGA, tend to underestimate band gaps. The high pressure hp1 phase becomes semiconductor at the phase transition point and the calculated E_g is around 1.1 eV. On the other hand, the hp2 phase becomes metallic. This finding is consistent with the recent electrical resistance measurements[14] where from the color change it was found that AlH_3 becomes semiconducting around 60 GPa and it further transforms into metal at ca. 100 GPa.

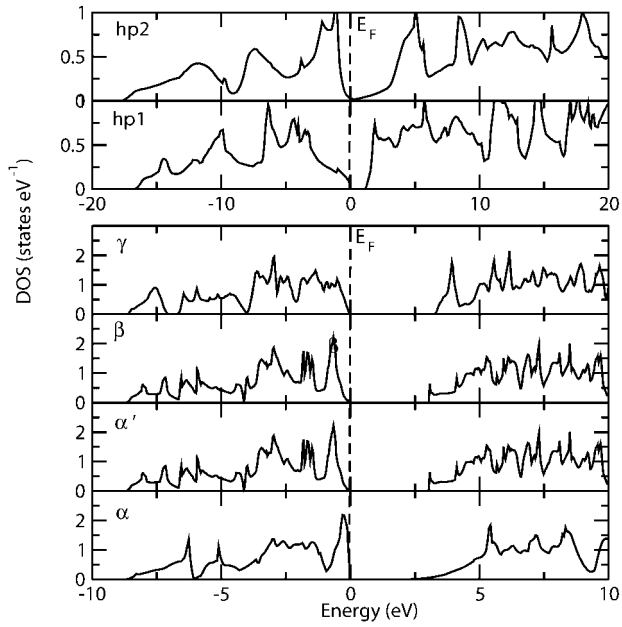

Figure 4. Calculated total density of states for AlH_3 in different polymorphs. The modifications are noted in the corresponding panel, and the Fermi level is set at zero energy.

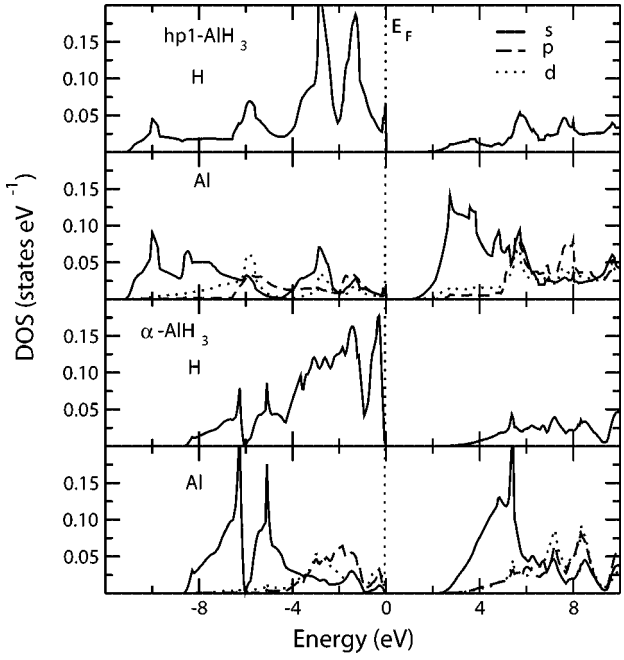

Figure 5. Calculated partial density of states for α- and hp1-AlH_3. The modifications are noted in the corresponding panel, and the Fermi level is set at zero energy.

Overall, the total DOS among these six phases, α, α′, *β*, and *γ*, have almost similar features (see Figure 4): i.e., the valence band of Al 3p character is at almost the same energy level as that of H 1s; their shapes are also similar (see Figure 5). This indicates that all these phases may have similar bonding character. On the other hand, in the hp1 and hp2 phases, the calculated DOS are significantly different from that of other phases mentioned above. Figure 5 clearly indicates that the Al s and p states are well-separated in the α-AlH_3 phase and the Al p states are present between −4 and 0 eV in the valence band. In contrast, due to the Al sp hybridization in hp1 phase, the Al s and p states are spread

over the VB region. This is the main reason why the Al p states are systematically moved to lower energy region, and this phase has long Al−H (1.8 Å) distances compared to the other polymorphs except the from hp2 phase. Because of the long Al−H distances, the DOS of the H s state become narrow (see Figure 5) compared to the ambient and low pressure phases.

It will be interesting to note that, in general, it is widely believed that the cubic modifications may have lower decomposition and better kinetics than the other modification. This is at least true in the case of MgH_2 where the cubic Mg_7TiH_x has lower decomposition than the TiH_2 and MgH_2.[24] Further more, it is evident that one can stabilize the high pressure polymorph of MgH_2 by transition metal substitution.[25] In this aspect one can expect the hp2 polymorph of AlH_3 may stabilize in this way and it may also have lower decomposition than the other AlH_3 modifications. So, the identification of cubic high pressure phase has implications to the hydrogen storage applications.

In summary, the stability of AlH_3 has been studied up to 175 GPa using density-functional total-energy calculations. At ambient pressure, AlH_3 stabilizes in the β-FeF_3-type structure. Similar to obtaining various modifications of AlH_3 by different preparatory conditions, one can also obtain these modifications by application of pressure. Application of pressure transforms β phase into four different modifications. The calculated structural data for α, α', β, and γ modifications are in very good agreement with experimental values. At equilibrium, the energy difference between these modifications is very small, and as a result, depending upon method of synthesis one can stabilize these phases at ambient conditions. Application of pressure changes the coordination of Al from 6 (α, α', β, and γ) to 9 (hp1) to 12 (hp2). The electronic structure reveals that AlH_3 remains nonmetal up to 60 GPa, more pressure makes it semiconducting. On further application of pressure, AlH_3 becomes metallic at ca. 106 GPa. Two new high pressure modifications were predicted, and during the revision of the present work, one of the predicted high pressure modifications [hp2 ($Pm\bar{3}n$)] has been confirmed experimentally. Additional high pressure experimental studies are needed to confirm the predicted high pressure modification [hp1 ($P63/m$)] also at the intermediate pressure range.

Acknowledgment. The authors gratefully acknowledge the Research Council of Norway for financial support and for computer time at the Norwegian supercomputer facilities.

CM800282B

(24) Kyoi, D.; Sato, T.; Rönnebro, E.; Kitamura, N.; Ueda, A.; Ito, M.; Katsuyama, S.; Hara, S.; Noréus, D.; Sakai, T. *J. Alloys Compd.* **2004**, *372*, 213–217.

(25) Vajeeston, P.; Ravindran, P.; Fjellvåg, H.; Kjekshus, A.; Noréus, D. in press.